

MULTI-COLOR LASER INDUCED FLUORESCENCE LIDAR

A DISSERTATION PROPOSAL SUBMITTED TO MY DISSERTATION  
COMMITTEE

By  
Troy T. Hix

July 27, 2006  
Version 0.4.4

# Chapter 1

## Laboratory Tests and Apparatus Development

In this chronologically organized chapter, the measurements that facilitate the development of the experimental apparatus are described. The first measurement described is a broadband absorption experiment conducted in November 2003. The basic data acquisition instrumentation is assembled and a first generation iodine cell is tested. The development continues up to a measurement of the LIF from solid anthracene conducted in March 2006 when the “ghost lines” from the grating in the 1 m monochromator are revealed. For each measurement the resulting contributions toward instrumentation are highlighted.

The loading system for a custom re-loadable sample cell is not complete and will not be included here. Experiments at various buffer gas pressures will be conducted when the system is ready; however, multi-color single-mode experiments await capable laser systems. Current efforts are centered on the production of single mode high power pulsed output using a tunable diode laser “idler” source amplified with a YAG pumped dye cell.

Reference [?] presents the absorption and LIF spectrum of molecular iodine. In this work we measure the absorption spectrum using LED’s instead of a white light source and we generate the LIF spectrum using green HeNe output and dye laser output instead of red HeNe output. Reference [?] reports the quenching of the total iodine fluorescence signal and [?] measures the lifetime of individual LIF features; however, these measurements were conducted at low pressure (0.03 Torr). In this work we look at the decay of a single LIF line at relatively high pressures.

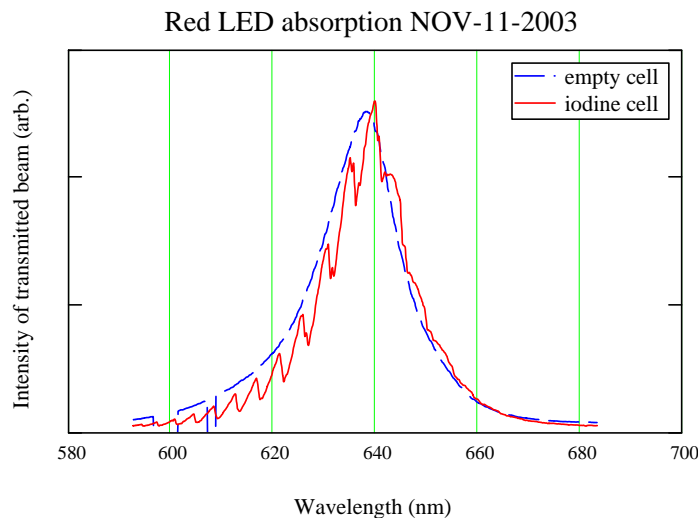


Figure 1.1: Red LED absorption in molecular iodine. The solid trace is about 2 times smaller than the dashed trace

## 1.1 Preliminary tests

One of the simplest fundamental spectroscopy experiments is bulk absorption. Here we describe a basic absorption experiment using low cost light sources which were immediately available: light emitting diodes (LED). The LEDs response to the high voltage output of a Hg wetted relay was measured. This allowed the development of the Hg pulser system and a fast photodiode. Finally HeNe based LIF measurements are used to vet two different beam line geometries, as well as test the Hg pulser/Pockels cell system.

### 1.1.1 Broadband molecular iodine absorption

We measure the broadband absorption spectrum of molecular iodine using LED illumination. Three LED's were used: red (see Figure 1.1), yellow (see Figure 1.2), green (see Figure 1.3). The absorption features match those in the literature in shape and spectral position. Also the general observation that iodine exhibits heavier absorption in the green than the red is supported by the data.

As one of the first measurements recorded, these experiments were used to develop the essential components of this spectroscopic study: spectral analysis, light detection, data acquisition, light sources, and sample preparation. A side-view PMT is mounted at the monochromator output and encased in an aluminum foil lined cardboard box; this

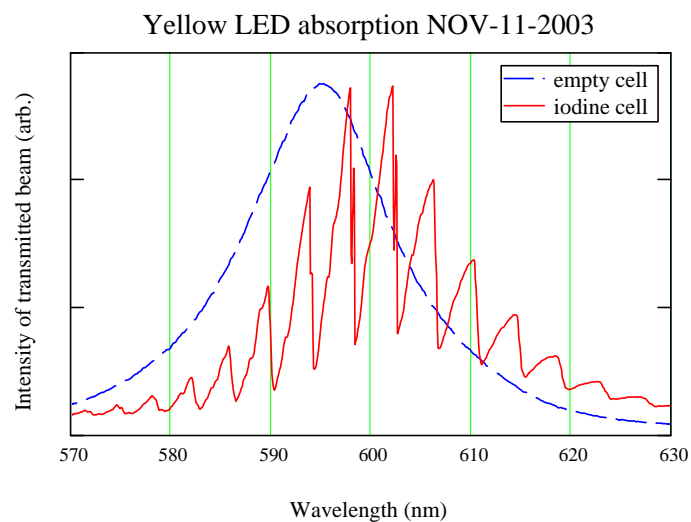


Figure 1.2: Yellow LED absorption in molecular iodine. The solid trace is about 5 times smaller than the dashed trace

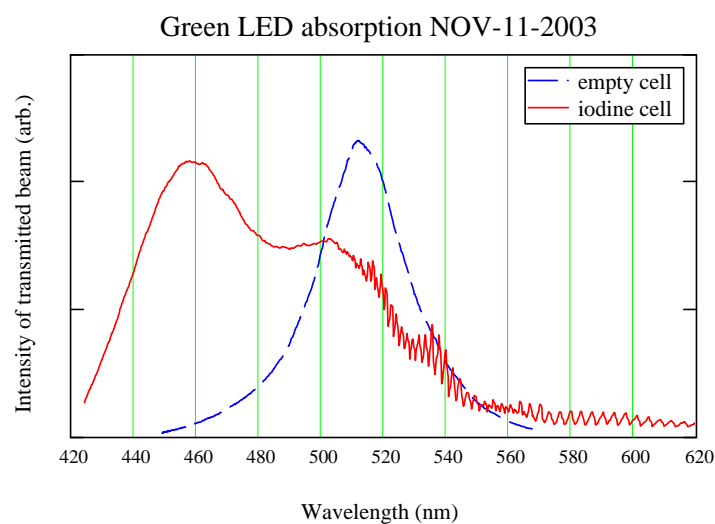


Figure 1.3: Green LED absorption in molecular iodine. The solid trace is about 10 times smaller than the dashed trace

primitive setup proves very reliable. A chart recorder is used to acquire data; the pen axis is “linearly” scanned using a voltage rise from a simple RC circuit. Data processing methods are developed to account for the non-linearity of the voltage rise. Gas lamp calibration procedures are developed for use with the monochromator.

A cell is prepared in a crude fashion by simply loading a sample cell with a few flakes of iodine in an unprotected environment (outdoors, in front of the physics building), closing the cell’s greased stop cock, connecting the cell to a mechanical vacuum pump, and evacuating the loaded cell at room temperature. The cell is closed off again, wrapped in heat tape, and temperature stabilized at 150° F with a bench top controller and used on the optical bench. Ideally at this temperature the overloaded iodine cell should have a collision lifetime of 11 ns, a density of  $1.9 \times 10^{17}$  molecules/cm<sup>3</sup>, and a pressure of 6.8 Torr (from an internal AHI document DN-3300-4 by Dr. Pui K. Lam). The cell is wrapped in aluminum foil giving it a “baked potato” appearance – hereafter, this cell will be referred to as such.

### **1.1.2 Boxcar averager and Hg pulser**

Some of the LED absorption data were taken by pulsing the LED (using an HP model 8015A pulse generator) and averaging the PMT signal with a boxcar averager (PAR, model CW-1). The goal of this experiment is to determine the usability of the donated averager; it is determined that the averager is unusable in its present state. This prompted the purchase of a new boxcar averager system.

To check the performance of a high voltage fast rise time mercury wetted relay (C.P. Clare & Co., model HGSS 5060, called “Hg pulser” hereafter – see UH notebook UH-004 pages 49–53) and test the performance of a newly assembled fast photodiode (see UH notebook UH-015 pages 7–48), the LED’s used here were connected to the output of the relay and the resulting signal observed using the fast photodiode. The relay itself is found to perform faster than the response time of the scopes available in the lab. The LED tested can take at least 100 V in a 20 ns pulse without damage; however, it is found to have a slower response than the relay output. This may be due to the coupling between the LED and the signal cable.

### **1.1.3 Red and green HeNe LIF**

Measurements of LIF from molecular iodine illuminated with red and green HeNe can be found in the literature and are performed in undergraduate labs. We repeat some

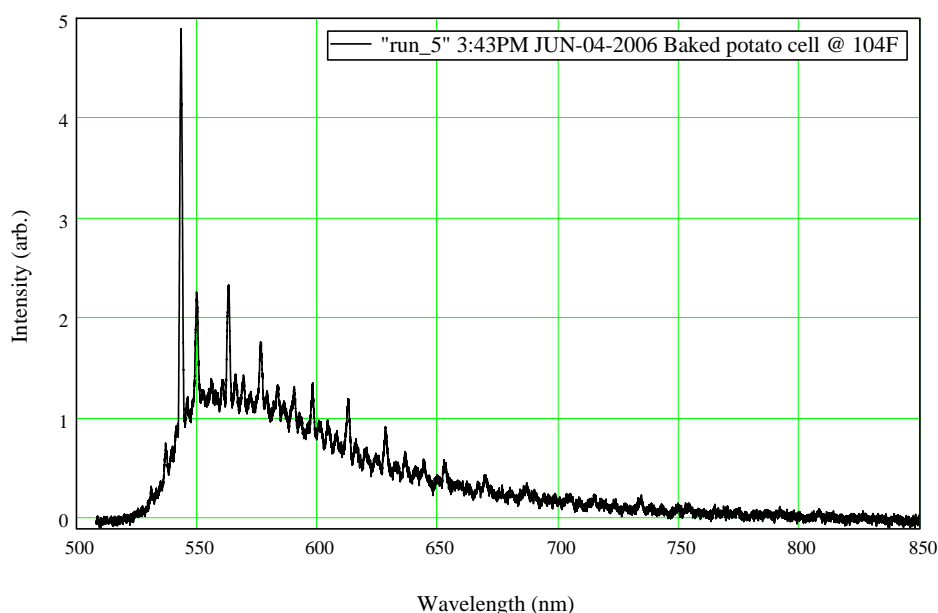


Figure 1.4: Red HeNe LIF from the “baked potato” iodine cell. Notice the broad pedestal absent in the “clean” cell scan in Figure 1.5 – see Section 1.2.2 for discussion.

of these experiments to verify the calibration procedures to acquire spectral data and the numerical model use to analyze these data. See Figures 1.4 and 1.5 for scans of a crudely prepared iodine cell and a scan from a commercially prepared cell.

The high voltage fast rise time relay mentioned in Section 1.1.2 will be used to provide the fast voltage pulse that will drive the Pockels cell in the final dye laser system. The simple beam line used for the LIF measurement mentioned above is exploited to test a recently acquired Pockels cell (Cleveland Crystals Inc., Impact 8 KD\*P Pockels Cell with a 532 nm AR coating). A crude Pockels cell mount is quickly constructed and the red HeNe output is sent through two crossed polarizers with the Pockels cell mounted in between. Alignment proved difficult (this knowledge prompted the design and construction of a new Pockels cell mount); however, once setup properly, the Pockels cell/Hg pulser system worked well (see Sections ?? and ?? or UH notebook UH-015 page 59).

## 1.2 Dye laser test

This section describes three experiments mainly used to check the performance of the dye laser system (Sirah Laser model PRSC-D-24). A wavelength scanned absorption experiment reveals some problems with the mechanical systems in the dye laser. Resonant LIF from a quickly prepared cell confirms the trial molecule was a good choice and provides

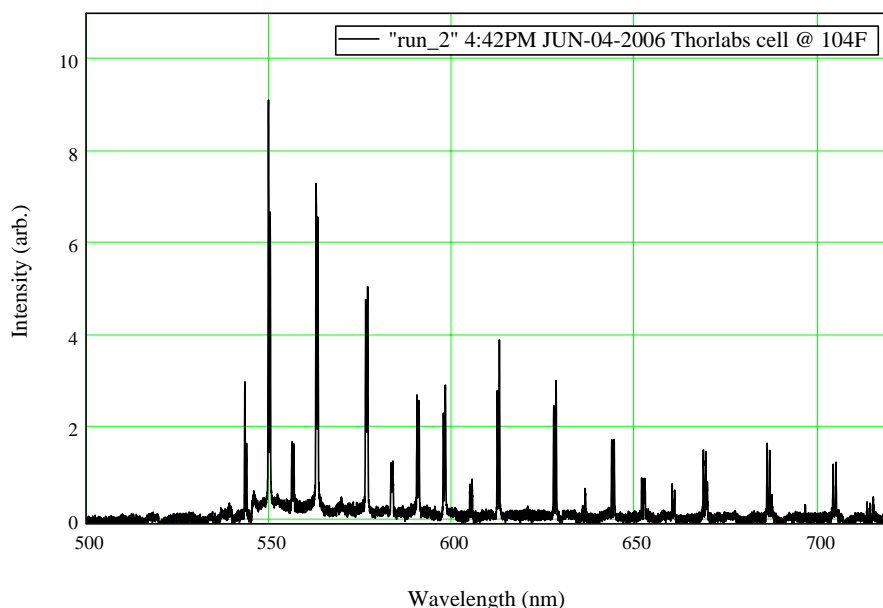


Figure 1.5: Red HeNe LIF from a “clean” commercial iodine cell (Thorlabs)

an opportunity to develop an automated computer based data acquisition system. Scanning the dye laser wavelength in a region containing two absorption peaks and observing the resulting fluorescence signal at high resolution reveals a subtle calibration issue and demonstrates one of the key issues in molecular discrimination: the high transition density of these systems.

### 1.2.1 Dye laser absorption in molecular iodine

The spectral region around a targeted absorption feature is scanned in a stepwise fashion (the wavelength “scan” feature of the dye laser has proven unrealizable) using the “lambdalok” feature of the dye laser. These scans will be referenced later when we observe LIF from excitation in this region.

The output of the dye laser is sent through three attenuation tools before going through the “baked potato” sample cell. The 13 mJ beam from the dye laser [see UH notebook UH-016 pg 62)] is reduced by a factor of  $4^3$  after the attenuation tools [see UH notebook UH-015 pg 117)] for an incident energy of 200 uJ in each 8 ns pulse at 20 Hz. The beam which passes through the cell is detected with a photodiode and averaged with a boxcar integrator then tabulated as a function of dye laser wavelength.

The output of the boxcar averager is connected to the vertical axis of a chart recorder. At each “lambdalok” setting the vertical position of the pen is recorded after

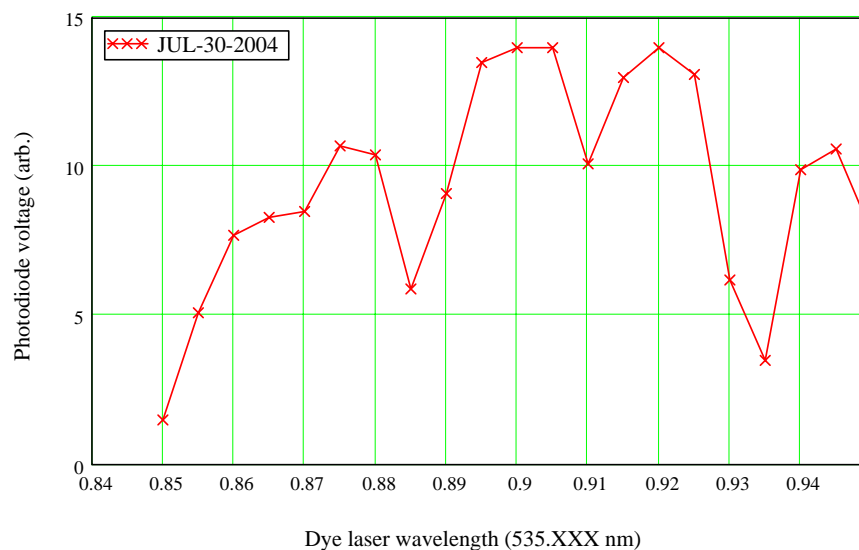


Figure 1.6: Iodine absorption dye laser scan. The fluctuations were about  $\pm 20\%$  of the value on the vertical scale (see UH notebook UH-016 page 9).

the boxcar output stabilizes (the experimental repetition rate is 20 Hz and the “samples” setting on the averager is set to 300). See Figure 1.6 for a plot of these data. The absorption peak (the “peak” points down) near 535.885 nm is the focus of the following discussion.

There are two transitions under investigation in this study. The first is the transition between the  $\nu'' = 0$ ,  $J'' = 52$  state in the X band to the  $\nu' = 30$ ,  $J' = 51$  state in the B band, called “transition one” hereafter. The second is the transition between the  $\nu'' = 0$ ,  $J'' = 55$  state in the X band to the  $\nu' = 30$ ,  $J' = 56$  state in the B band, called “transition two” hereafter.

Transition one has an excitation energy corresponding to 535.8843 nm while transition two has an excitation energy corresponding to 535.8901 nm. The resolution of the scan is high enough to identify the absorption feature associated with these transitions; however, the individual transitions are not resolved and may indeed prove difficult to resolve with this scanning method. The goal of this exercise was not to identify specific peaks; instead, we simply seek to verify the performance of the dye lasers (again, it is discovered the “scan” feature was unreliable) and observe the basic absorption features of molecular iodine.

### 1.2.2 Resonant laser induced fluorescence

In this experiment the beam line is similar to the one described in Section 1.2.1 except here only one attenuation tool (measured pulse energy after the attenuator: 300  $\mu\text{J}$ )



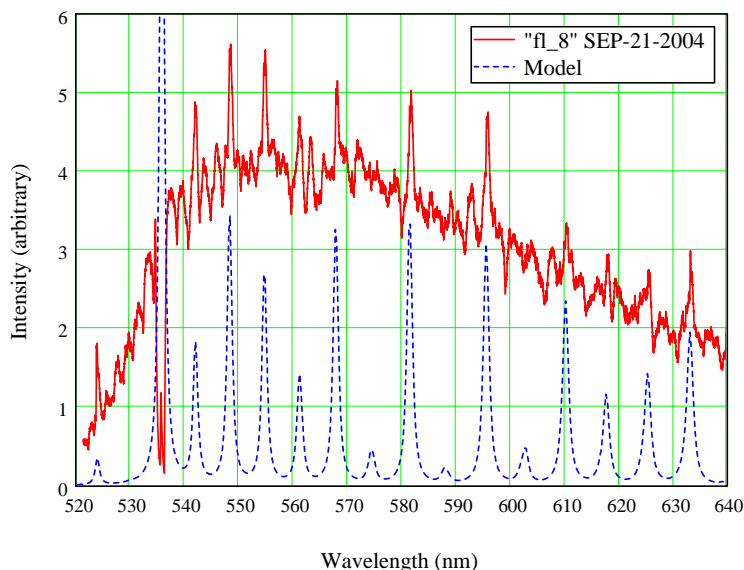


Figure 1.7: 535.8901 nm LIF from the “baked potato” iodine cell

is used and a +750 mm lens is placed 940 mm from the sample cell (between the sample cell and attenuation tool). The dye laser is tuned to 535.8901 nm and a side view geometry is used with a +100 mm object lens and a +500 mm image lens to collect the fluorescence radiation into a 1 m grating monochromator. A PMT is used to detect the signal at the monochromator output and a boxcar integrator is used to amplify/average the signal.

While targeting transition two (see Section 1.2.1) with the dye laser (wavelength set at 535.8901 nm), the boxcar output is recorded onto a computer while the monochromator is scanned from green to red. A 12.3 minute data run was recorded with the boxcar integrator “samples” setting at 30. The plot shows the raw data from the averager plus the numerical model output. During the wavelength scan a neutral density filter was inserted into the beam line to prevent PMT saturation (and possible damage) from the fundamental signal from the laser. This results in the discontinuity seen near 536 nm on the raw data trace (see Figure 1.7).

In general we have a large general spectral feature about 100 nm wide that “tails” off toward the red – this is typical of non-resonant fluorescence features, suggesting that the “baked potato” cell may have some contaminants (a reasonable conclusion). On top of the large feature are several distinct localized features corresponding to the resonant LIF response of molecular iodine. Comparing these features with the model calculation shows a close correspondence between the positions and relative heights of the peaks.

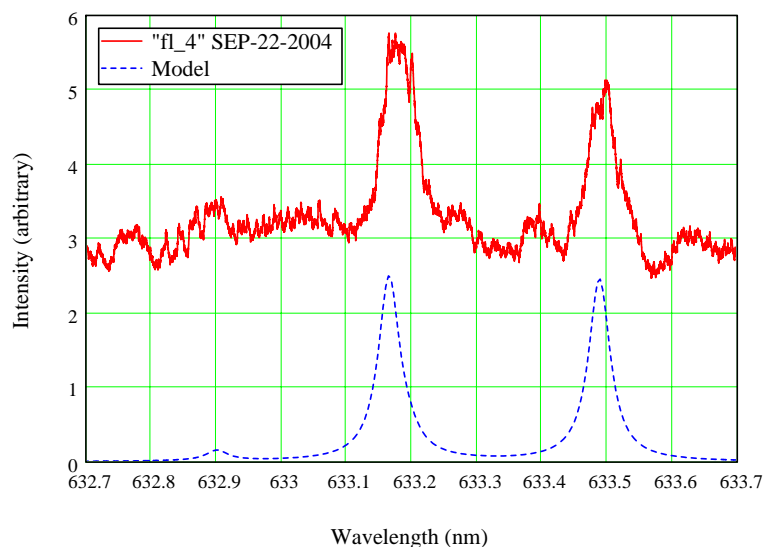


Figure 1.8: 535.8843 nm LIF (from “transition one”)

A major milestone in data acquisition development is reached in this test. The computer interface (Stanford Research Systems model SR245) purchased with the new boxcar system is introduced into the apparatus. LabView control software is written to simulate “chart recorder” type data acquisition; the data plotted in Figure 1.7 is one of the first data set acquired using the SR245.

### 1.2.3 Transition selection

The dye laser system maintains enough control of its output spectrum to allow discrimination between a target transition and its nearest strong neighbor. There may be some remaining calibration issues, but the numerical model for iodine LIF does a good job of modeling the observed spectral features in the LIF spectrum. Transition one and two (see Section 1.2.1) are selected by tuning the dye laser to their respective wavelengths and the resulting fluorescence spectra are observed.

The beam line used for these data is identical to the one described in Section 1.2.2 except two attenuation tools are used so that the energy after the attenuators is 120 uJ. The “lambdalok” feature on the dye laser is used to set the dye laser to within a claimed 2 pm of the set wavelength. Resulting iodine fluorescence spectrum features are analyzed and recorded for various excitation wavelengths.

The fluorescence feature near 633 nm is shown in Figures 1.8 and 1.9. The basic characteristics of the feature is its “paired” nature. Two lines representing the  $J = \pm 1$

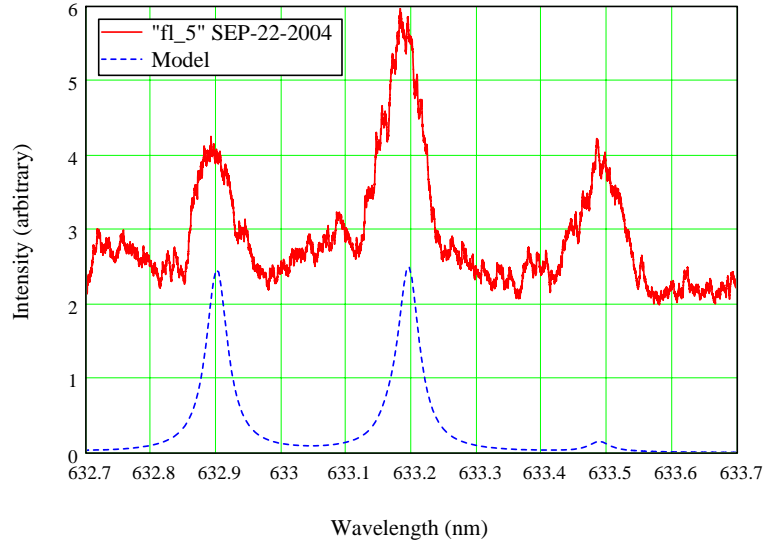


Figure 1.9: 535.8901 nm LIF (from “transition two”)

transitions (see Section ??) are clearly resolved in these data. The pair at 633.17 nm and 633.49 nm are associated with transition one (535.8843 nm). The pair at 632.90 nm and 633.20 nm are associated with transition two (535.8901 nm). See Figure 1.8 for the resulting features when the laser is tuned for 535.8843 nm and see Figure 1.9 for the resulting features when the laser is tuned for 535.8901 nm.

At first glance it seems that transition one was hit well and transition two was not. According to the model, the excited transitions (535.8843 nm and 535.8901 nm) should result in fluorescence with roughly the same intensity in the spectral window under consideration. Inspection of Figures 1.8 and 1.9 shows that the non-overlapped line (the right most line in Figure 1.8 and the left most line in Figure 1.9) do not have the same heights. In fact the data plotted in Figure 1.9 are consistent with excitation somewhere between transition one and two. This may be the result of a 3-4 pm shift in the calibration of the dye laser and/or the “lambdalok” feature performing below specification. And, since these transitions are separated by 6 GHz, it indicates that selective excitation can be difficult due to the relatively broad dye laser spectrum.

### 1.3 Single fluorescence line decay

Decay processes play a major role in this study. The target is assumed to be a relatively unprepared region of atmosphere; thus, in the actual application, we will have little

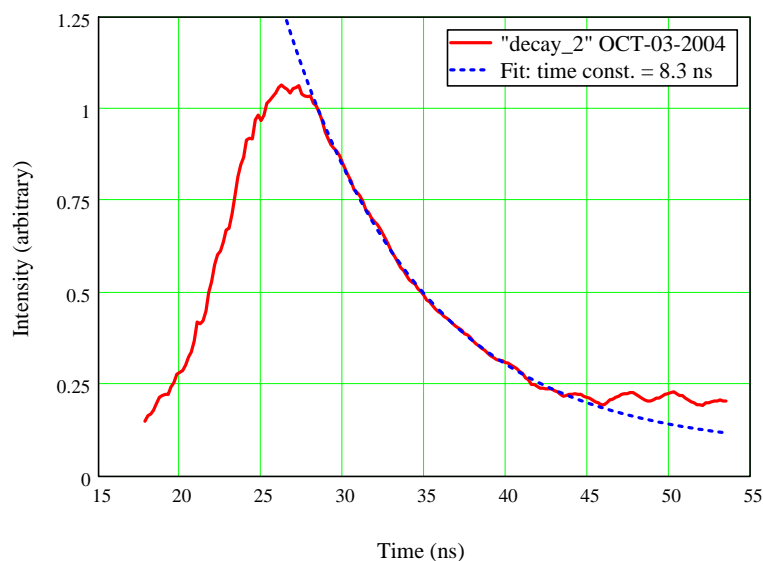


Figure 1.10: Decay of 535.893 nm LIF line at 632.9 nm (cell at 150° F). The decay rate is inconsistent with the ideal calculation from Section 1.1.1; however, considering the likely contamination of the cell (see Figures 1.4 and 1.7 and the associated discussion in Section 1.2.2

direct control of the parameters that influence the system relaxation. In the experiments leading up to the field demonstration, controlled samples will be used. Here we conduct an initial measurement of the lifetime of a single LIF feature using the “baked potato” iodine cell.

### 1.3.1 Pockels cell system integration

Integration of the Pockels cell into the dye laser system requires the design and assembly of a trigger/delay system used to trigger the YAG pump and delay the activation pulse to the Pockels cell until the incident dye laser pulse arrives at the Pockels cell location (see UH notebook UH-016 pages 56–59). The system consists of three signal generators (HP model 8015A pulse generators), a high voltage DC power supply to charge the Hg pulser (HP model Harrison 6525A), and the associated delay cables and attenuators. The Pockels cell is placed between two polarizing cube beam splitters.

### 1.3.2 Single fluorescence line decay in molecular iodine

There are several non-radiative decay mechanisms which can lead to an observed damping of the fluorescence lifetime of a single LIF line. The iodine molecule can dissoci-

ate, ionize (once, twice,...), internally decay via a non-optical transition, exchange energy through inelastic collisions, or de-phase through elastic collisions. In Section ?? we modeled de-phasing through collisions in a stochastic manner. Here we directly measure the observed decay of a LIF line in the “baked potato” iodine cell.

The beam line used here is similar to the one described in Section 1.2.2 except the attenuators are not used and in its place we use a pair of crossed polarizers (polarizing cube beam splitters) and a Pockels cell. The system has an extinction ratio of about 200:1 (see UH notebook UH-018 page 65) and produces a pulse with a FWHM of about 4 ns. Before the Pockels cell we have about 5.4 mJ, thus after the Pockels cell (heading toward the +750 mm lens) is about 27 uJ. The dye laser is tuned to 535.893 nm (a targeted absorption line) and the monochromator is tuned to capture a single LIF line at 632.9 nm. Again the signal from the PMT at the output of the monochromator is scanned (temporal gate scan) and averaged with a boxcar averager.

The measurement has facilitated the development of the data acquisition system required for lifetime measurements. The boxcar averager works at the 1000 ps gate width setting (it has settings down to 100 ps, but these have not been tried) and the LabView program records the data as a convenient text file. We have also discovered that the intensity fluctuations of the dye laser output introduce unwanted jitter in the position of the trigger relative to the peak – accurate lifetime measurements will require a way to eliminate the jitter or, better yet, reduce the intensity fluctuations in the input beam. Contamination of the cell may have introduced additional channels through which the iodine can decay. A clean loading method must be developed in order to isolate and measure specific effects on the fluorescence decay.

## 1.4 Aromatic compound LIF

Iodine is the trial system used to form the computational basis of many of the claims made in this dissertation. The scope of this general study and the development of the experimental equipment go beyond the iodine molecule; this section describes an experiment using naphthalene as a target. Temperature controlled sample cells containing naphthalene have been prepared along with flakes of naphthalene and anthracene. An attempt to observe a multi-photon process in these aromatic samples has led to more equipment development.

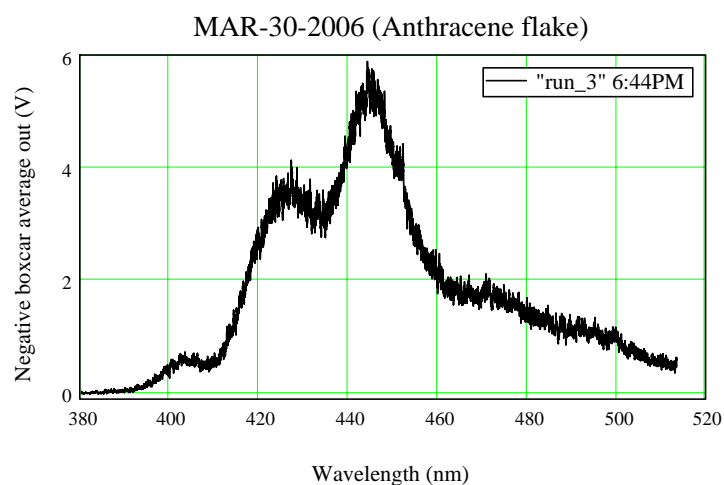


Figure 1.11: LIF from a solid anthracene flake illuminated by a 355 nm YAG

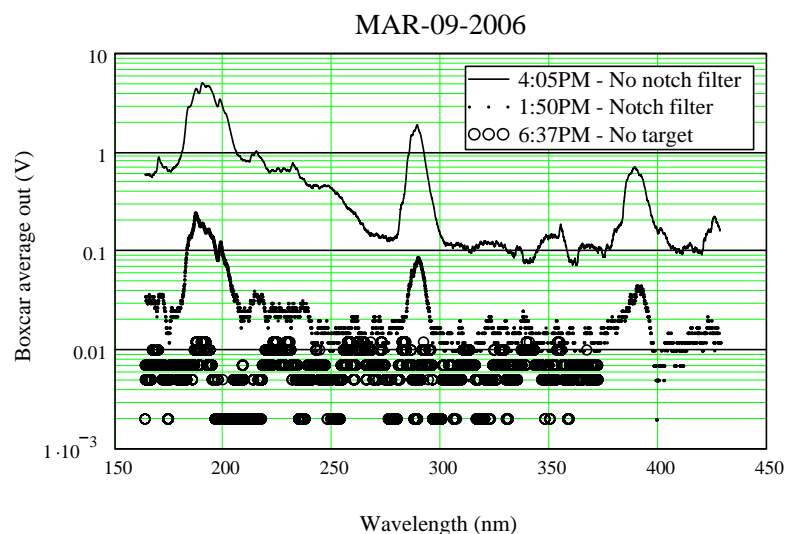


Figure 1.12: Grating ghosts from 1064 nm laser illumination. Using various targets (aromatic compounds, paper, and a calibrated Lambertian target) it was discovered that the spectral “features” observed in the UV were independent of the target. Then from the data shown here, acquired using a notch filter made for 1064 nm YAG output, it was concluded that the “features” were linearly related in intensity to the 1064 nm excitation and thus most likely “ghost lines” associated with the grating.

Measurements of the fluorescence response of aromatic compounds to YAG illumination have revealed some shortcomings of the 1 m monochromator. Figure 1.11 shows the LIF from an solid anthracene sample when excited by the output of a tripled Nd:YAG laser (355 nm). When the excitation is shifted to the doubled or fundamental output of the YAG, a complicated faint spectrum emerges in the scans. It was discovered that the faint features were independent of the target (paper and a white Lambertian target generated the same features). See Figure 1.12 for the ghost lines resulting from fundamental YAG (1.06  $\mu\text{m}$ ) illumination. It is believed that these are “ghost lines” from sub-periods in the groove spacing [?]. A holographic replacement grating (which should be free of ghost lines) is being procured.

## 1.5 Conclusion

This chapter chronicles the stages of laboratory development undergone over the past few years. The main measurements at each stage were used as a guide to develop the equipment and techniques required for demonstration of molecular control in LIDAR systems.

As each stage was completed various components of the apparatus were either designed and assembled or evolved to the next generation. After the installation of the PMT at its output the monochromator served each experiment well until the recent aromatic compound measurements. The Hg pulser and Pockles cell system went through various stages of development starting with the initial tests of the Hg pulser on LED’s to the integration of the system with the YAG pumped dye laser system during the fluorescence line decay measurements. The software model was tested at each stage from the familiar non-resonant HeNe LIF to pulsed resonant dye LIF. The data acquisition system was built for the first dye laser experiments and has remained relatively unchanged since then. Recently, a calibration issue with the monochromator self scan feature has prompted the need of a second generation of the data acquisition software.